

# SCIENTIFIC REPORTS

OPEN

## A *Drosophila* Model of Essential Tremor

Philip Smith<sup>1</sup>, Ronald Arias<sup>2</sup>, Shilpa Sonti<sup>2</sup>, Zagaa Odgerel<sup>2</sup>, Ismael Santa-Maria<sup>2</sup>, Brian D. McCabe<sup>3</sup>, Krasimira Tsaneva-Atanasova<sup>4,5</sup>, Elan D. Louis<sup>6,7,8</sup>, James J. L. Hodge<sup>1</sup> & Lorraine N. Clark<sup>2,9</sup>

Received: 27 June 2017

Accepted: 25 April 2018

Published online: 16 May 2018

Essential Tremor (ET) is one of the most common neurological diseases, with an estimated 7 million affected individuals in the US; the pathophysiology of the disorder is poorly understood. Recently, we identified a mutation (*KCNS2* (*Kv9.2*), c.1137T > A, p.(D379E) in an electrically silent voltage-gated K<sup>+</sup> channel  $\alpha$ -subunit, *Kv9.2*, in a family with ET, that modulates the activity of Kv2 channels. We have produced transgenic *Drosophila* lines that express either the human wild type *Kv9.2* (h*Kv9.2*) or the ET causing mutant *Kv9.2* (h*Kv9.2*-D379E) subunit in all neurons. We show that the h*Kv9.2* subunit modulates activity of endogenous *Drosophila* K<sup>+</sup> channel *Shab*. The mutant h*Kv9.2*-D379E subunit showed significantly higher levels of *Shab* inactivation and a higher frequency of spontaneous firing rate consistent with neuronal hyperexcitability. We also observed behavioral manifestations of nervous system dysfunction including effects on night time activity and sleep. This functional data further supports the pathogenicity of the *KCNS2* (p.D379E) mutation, consistent with our prior observations including co-segregation with ET in a family, a likely pathogenic change in the channel pore domain and absence from population databases. The *Drosophila* h*Kv9.2* transgenic model recapitulates several features of ET and may be employed to advance our understanding of ET disease pathogenesis.

Recent studies suggest that ET could be a neurodegenerative disorder, primarily affecting the cerebellar system, accompanied by changes in the Purkinje cell population and altered (i.e. reduced) brain GABA tone<sup>1</sup>; however, this is far from established. Recently, we identified a mutation in the *KCNS2* gene (*Kv9.2*, c.1137 T > A, p.(D379E), encoding an electrically silent voltage-gated K<sup>+</sup> channel  $\alpha$ -subunit, *Kv9.2*, in a single family with early-onset ET<sup>2</sup>. The *KCNS2* mutation cosegregated with ET in this family and was present in all four affected individuals and absent in an unaffected family member.

*KCNS2* encodes an electrically silent voltage-gated K<sup>+</sup> channel  $\alpha$ -subunit, *Kv9.2*, that is highly and selectively expressed in the brain and modulates the activity of the Kv2.1 and Kv2.2 channels by heteromultimerization. A similar localization of expression of *Kv9.2* with Kv2.1 and Kv2.2 has been observed in the Purkinje and granular cells in mouse cerebellum<sup>3</sup>.

In *Drosophila*, voltage gated potassium ion (Kv) channels play a major role in regulating membrane excitability and synaptic transmission in many central neurons and at the neuromuscular junction (NMJ)<sup>4</sup>. Thus, *Drosophila* is a useful model system for investigating ion channel kinetics and their impact on neuronal firing properties. A direct ortholog of *Kv9.2* is absent from *Drosophila* with the closest homologue to *Kv9.2* in *Drosophila* being *Shab* (42% amino acid identity and 63% amino acid similarity). The *Drosophila* genome encodes four prototypic members of the Kv channel gene family, namely, *Shaker* (*Kv1*), *Shab* (*Kv2*), *Shaw* (*Kv3*), and *Shal* (*Kv4*)<sup>5</sup>. In *Drosophila* neurons *Shab* encodes the majority of delayed rectifier current (I<sub>k</sub>) and is a member of the Kv2 subfamily<sup>5,6</sup>. *Drosophila* *Shab* I<sub>k</sub> is important in the regulation of high frequency repetitive synaptic activity and removal of

<sup>1</sup>School of Physiology, Pharmacology and Neuroscience, University of Bristol, University Walk, Bristol, BS8 1TD, UK. <sup>2</sup>Department of Pathology and Cell Biology, College of Physicians and Surgeons, Columbia University, New York, NY, 10032, USA. <sup>3</sup>Brain Mind Institute, Swiss Federal Institute of Technology (EPFL), Lausanne, Switzerland. <sup>4</sup>Department of Mathematics and Living Systems Institute, University of Exeter, Stocker Road, Exeter, EX4 4QD, UK. <sup>5</sup>EPSRC Centre for Predictive Modelling in Healthcare, University of Exeter, Exeter, EX4 4QJ, UK. <sup>6</sup>Department of Neurology, Yale School of Medicine, Yale University, New Haven, CT, 06520, USA. <sup>7</sup>Center for Neuroepidemiology and Clinical Neurological Research, Yale School of Medicine, Yale University, New Haven, CT, 06520, USA. <sup>8</sup>Department of Chronic Disease Epidemiology, Yale School of Public Health, New Haven, CT, 06520, USA. <sup>9</sup>Taub Institute for Research on Alzheimer's Disease and the Aging Brain, College of Physicians and Surgeons, Columbia University, New York, NY, 10032, USA. Correspondence and requests for materials should be addressed to J.J.L.H. (email: james.hodge@bristol.ac.uk) or L.N.C. (email: lc654@columbia.edu)

Shab  $I_k$  dramatically increases NMJ transmission (up to 10-fold gain) during repetitive nerve stimulation<sup>4</sup>. The kinetics of the Shab channel are reported to be comparable to the classical (as described by Hodgkin–Huxley) delayed rectifier  $K^+$  channel<sup>6</sup>.

Abnormal motor behavior and leg shaking (with or without anesthesia) has been described in *Shab* mutant flies<sup>4</sup>. Many neurological disorders are associated with altered activity, function or expression of  $K^+$  channels<sup>7</sup> and mutations in these channels can cause cerebellar dysfunction and ataxia. Notably, a tremor phenotype has been described in patients with mutations in *KCNA1* (Kv1.1; EA; OMIM 160120)<sup>8</sup> and missense dominant negative mutations in *KCNC3* (Kv3.3) are associated with hyperexcitability, cerebellar neurodegeneration and subsequent movement defects including spinocerebellar ataxia (SCA13; OMIM 605259)<sup>9</sup>. Kv3.1 and Kv3.3 mutant mice also display severe motor deficits, including tremor, myoclonus, and ataxic gait and behavioral alterations that include constitutive hyperactivity and sleep loss<sup>10–12</sup>. In addition to inherited channelopathies, several neurodegenerative disorders including Alzheimer's disease, Parkinson's disease, Huntington's disease, amyotrophic lateral sclerosis, and SCAs exhibit altered properties of diverse  $K^+$  channels characterized by protein aggregate induced hyperexcitability (Kumar *et al.*<sup>13</sup>).

Currently, it is unclear how the mutation that we identified in Kv9.2 (p.D379E) could lead to an ET phenotype. However, the dominant inheritance pattern suggests a gain-of-function or dominant negative mechanism. To study the disease mechanism we have produced transgenic *Drosophila* lines that express either the wild type human Kv9.2 (hKv9.2) subunit or the ET causing mutant human Kv9.2 (hKv9.2-D379E) subunit in all neurons. Here, we show that the hKv9.2 subunit can modulate the channel activity of endogenous *Drosophila* Shab (Kv2), describe the behavioral manifestations of nervous system dysfunction, and the effects of hKv9.2 and hKv9.2-D379E on adult neuron activity.

## Results

To study the disease mechanism of the Kv9.2 (p.D379E) mutation that we identified in an ET family and advance our understanding of disease pathogenesis, we have produced transgenic *Drosophila* lines that express the wild type hKv9.2 or ET causing mutant hKv9.2-D379E subunit.

Pan-neural expression of the wild type hKv9.2 or mutant hKv9.2-D379E subunit resulted in no apparent gross morphological differences. Western blot analysis was used to verify transgenic expression of hKv9.2 and hKv9.2-D379E in *Drosophila*. Using a hKv9.2 immunogen corresponding to amino acids 175–470, we detected a 54.2 kDa band of the correct size corresponding to human hKv9.2 (Fig. S1).

**Behavioral Manifestations of Nervous System Dysfunction.** To test the hypothesis that mutations in Kv9.2 cause nervous system dysfunction, we tested the effect of pan-neural expression of hKv9.2-D379E compared to wild type hKv9.2 or controls on climbing response throughout the fly lifespan<sup>14</sup> (Fig. 1). Flies expressing either wild type or mutant human channels displayed significantly faster climbing ( $p < 0.0003$ ) throughout lifespan (Fig. 1A), consistent with the hKv9.2 channel expressing animals being behaviorally hyperexcitable as previously described for mutants of other Kv channels in locomotor assays<sup>15,16</sup>. Moreover, flies which only expressed the wild type or mutant hKv9.2 channel in adult neurons after development also displayed significantly faster climbing throughout lifespan ( $p = 0.04–0.0001$ ; weeks 3–5) suggesting that the phenotype is not due solely to changes during development (Fig. 1B).

Because ET is associated with increased mortality<sup>17</sup> and Kv channel dysfunction in both humans and flies is associated with disease and decreased lifespan (Kumar *et al.*<sup>13</sup>) we performed survival assays. Significant differences in lifespan were not detected between flies expressing hKv9.2 or hKv9.2-D379E channels during development compared to wild type (Fig. 2A). Flies expressing the wild type or mutant hKv9.2 channel post-developmentally in neurons however did display significant differences in lifespan compared to wild type (*Elav-gal4/+ Gal80<sup>ts</sup>* and *Elav-gal4 > Gal80<sup>ts</sup> hKv9.2* ( $p = 0.0012$ ) or *Elav-gal4/+ Gal80<sup>ts</sup>* and *Elav-gal4 > Gal80<sup>ts</sup> hKv9.2-D379E*. ( $p = 0.0001$ )). (Fig. 2B). The reduced lifespan observed for flies expressing the hKv9.2 or mutant hKv9.2 channel post-developmentally is consistent with a reduced lifespan observed for other hyperexcitable Kv channel mutants<sup>13</sup>.

Wing posture and motility deficits were also assessed. Normally, flies hold their wings flat and rarely display an elevated or downturned wing posture. However, we observed that approximately 40% of flies expressing hKv9.2 or hKv9.2-D379E pan-neuronally displayed an abnormal wing posture, with bilateral wing elevation, with onset 7–21 days post eclosion (Supplementary Movie 1). This abnormality may be due to muscle and/or neural based effects and a downturned wing phenotype has been described in other *Drosophila* models of neurodegeneration including Huntington's disease<sup>18</sup> and Parkinson's disease<sup>19,20</sup> and bilateral wing elevation has been described for flies expressing the ion channel gene, *TRPM8*, in adult neurons<sup>21</sup>. Alternatively this effect could also be due to a developmental effect or muscle based hyperexcitability as described in the *Drosophila ether-à-go-go* (*eag*) *Shaker* double mutant<sup>22</sup>. To test whether the abnormal wing posture observed in flies expressing hKv9.2 or hKv9.2-D379E pan-neuronally was due to a developmental effect we also assessed flies expressing the wild type or mutant hKv9.2 channel only in adult neurons. We observed that approximately 13% of flies expressing hKv9.2-D379E in adult flies displayed an abnormal wing posture, with bilateral wing elevation, with onset 6 weeks post eclosion ( $p < 0.0001$ ) (Fig. S2). Abnormal wing posture and motility defects were also observed in flies expressing the wild type hKv9.2 channel in post-developmental neurons (~20% also with onset 6 weeks after eclosion ( $p < 0.0001$ ) (Fig. S2)).

Hyperexcitable mutants such as *Shaker*, *Shab*, *Shaw*, *eag* and *Hyperkinetic* display abnormal leg shaking and wing scissoring in etherised adults<sup>23–25</sup>. Adult flies expressing hKv9.2 or hKv9.2-D379E pan-neuronally also exhibited leg shaking, abdominal pulsations and body shuddering under ether anesthetization (Supplementary Movie 2). The ether anesthetization induced tremor in these flies is consistent with reports in the literature of excitatory effects of commonly used anesthetics in humans that may manifest as spontaneous movements

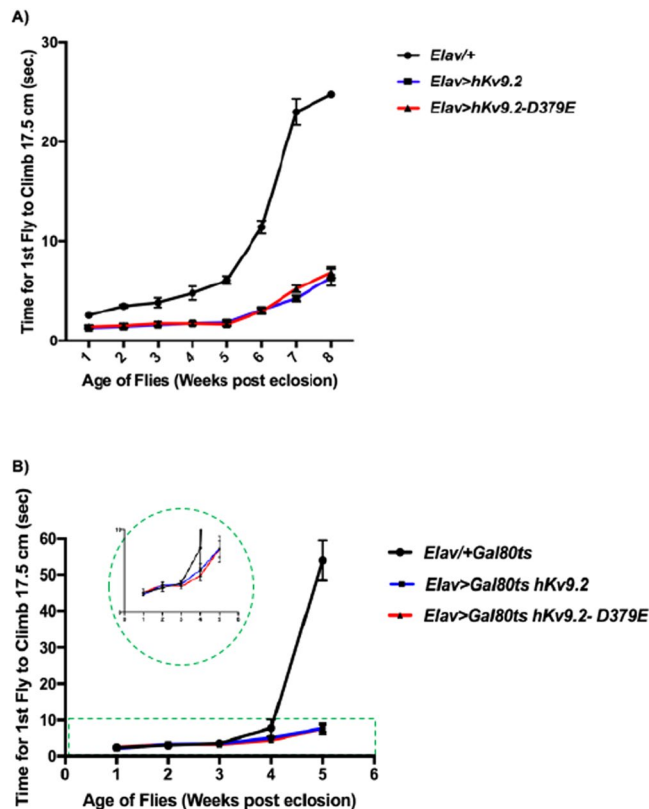


**Figure 1.** Climbing Response During Lifespan. The climbing index was assessed as the time taken for the first fly to climb 17.5 cm. (A) Expression of *hKv9.2* and *hKv9.2-D379E* channels throughout neuronal development and effects on climbing response during lifespan. The mean climbing index  $\pm$  SEM as a function of age is shown for *Elav*+/+, *Elav*>*hKv9.2* and *Elav*>*hKv9.2-D379E*. Each point represents the mean of 10 flies except for: Week 1, *Elav*>*hKv9.2* ( $n=9$ ); Weeks 1–8, *Elav*>*hKv9.2-D379E* ( $n=11$ ); Week 6, *Elav*+/+ ( $n=7$ ); Week 8, *Elav*+/+ ( $n=1$ ). Flies expressing either *Elav*>*hKv9.2* and *Elav*>*hKv9.2-D379E* displayed significantly faster climbing ( $p < 0.0003$ ) throughout lifespan. (B) Expression of *hKv9.2* and *hKv9.2-D379E* channels post developmentally in neurons and effects on climbing response during lifespan. The mean climbing index  $\pm$  SEM as a function of age is shown for *Elav-gal4*+/+ *Gal80*<sup>ts</sup>, *Elav-gal4*>*Gal80*<sup>ts</sup> *hKv9.2* and *Elav-gal4*>*Gal80*<sup>ts</sup> *hKv9.2-D379E*. Each point represents the mean of 10 or 9 flies. Flies expressing either *Elav*>*hKv9.2* and *Elav*>*hKv9.2-D379E* *Elav-gal4*>*Gal80*<sup>ts</sup> displayed significantly faster climbing ( $p = 0.04$ – $0.0001$ ; weeks 3–5) during lifespan.

including tremor, dystonia and myoclonus<sup>26</sup>. Interestingly, a number of observations suggest a link between anesthesia and ET, including an ET kindred with malignant hyperthermia<sup>27</sup> and a porcine model of malignant hyperthermia manifesting high frequency tremor<sup>28</sup>.

**Expression of either *hKv9.2* and *hKv9.2-D379E* causes an alteration in the kinetics of *Shab* (*Kv2*).** We determined the effects of *hKv9.2* and *hKv9.2-D379E* on neuron activity because ether anesthetization induced tremor in flies. *hKv9.2* and *hKv9.2-D379E* transgenes were expressed in flies and whole cell voltage clamp recordings were performed on the large lateral neuron ventral (l-LNV) clock neurons, which have been employed as model central neurons for electrophysiological measurements in *Drosophila*<sup>29,30</sup>. Using a *Shab* specific toxin we were able to isolate the *Shab* current (a voltage-sensitive non-inactivating  $K^+$  current) in these neurons consistent with previous reports<sup>6</sup>. Expression of either *hKv9.2* and *hKv9.2-D379E* in these neurons caused an alteration in the kinetics of *Shab* (*Kv2*) (Fig. 3A). The current evoked from *Shab* when depolarized from  $-133$  mV to  $-3$  mV showed that the non-inactivating *Shab* becomes inactivating in the presence of the wild type *hKv9.2* subunit and to a greater extent with the mutant *hKv9.2-D379E* subunit (Fig. 3A). The I-V relationships for *Shab* in the three given genotypes was also determined (Fig. 3C). The peak current shows that expression of the *hKv9.2* subunits cause a shift in activation of *Shab* to more negative voltages. The sustained current shows that, at similar voltages, flies expressing either *hKv9.2* subunit show reduced *Shab* current after 200 ms of depolarization. When the sustained current after 200 ms of depolarization is expressed as a percentage of the peak current the flies with only native *Shab* (i.e. controls) show high percentages, indicating very low levels of inactivation (Fig. 3C). Flies expressing either the wild type *hKv9.2* subunit ( $p < 0.001$ ) or the mutant *hKv9.2-D379E* subunit ( $p < 0.001$ ) were significantly different to flies with only endogenous *Shab* alone (control). Comparing the relative sustained currents (Fig. 3C), the mutant *hKv9.2-D379E* subunit shows significantly higher levels of inactivation than the wild type *hKv9.2* subunit ( $n = 3$ ,  $p = 0.0438$ ). The observed change in the inactivation kinetics of *Shab* in the presence of mutant *hKv9.2-D379E* subunit would be predicted to result in neuronal hyperexcitability.

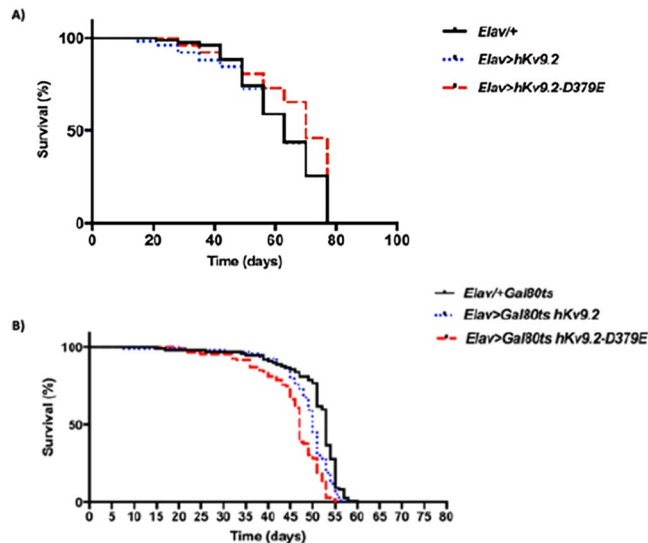


**Figure 2.** Lifespan Assays in hKv9.2 Transgenic Lines. **(A)** Expression of hKv9.2 and hKv9.2-D379E channels throughout neuronal development and effects on lifespan. A total of 200 virgin flies per line were sex-segregated within 4 h of eclosion and maintained in small laboratory vials ( $n = 20$  per vial) containing fresh food in a low-temperature incubator at 25 °C and 40% humidity on a 12/12 h dark/light cycle. The flies were then transferred to fresh food vials every 3–4 days and mortality recorded. Significant differences were not observed between *Elav/+* and *Elav > hKv9.2* ( $p = 0.8771$ ) or *Elav/+* and *Elav > hKv9.2-D379E* ( $p = 0.0656$ ). **(B)** Expression of hKv9.2 and hKv9.2-D379E channels post developmentally in neurons and effects on lifespan. A total of 100 virgin flies per line were sex-segregated within 4 h of eclosion and age-matched flies were maintained in small laboratory vials ( $n = 10$  per vial) containing fresh food in a high-temperature incubator at 29 °C and 40% humidity on a 12/12 h dark/light cycle. The flies were then transferred to fresh food vials every 2–3 days and mortality recorded. Significant differences were observed between *Elav-gal4/+Gal80<sup>ts</sup>* and *Elav-gal4 > Gal80<sup>ts</sup> hKv9.2* ( $p = 0.0012$ ) or *Elav-gal4/+Gal80<sup>ts</sup>* and *Elav-gal4 Gal80<sup>ts</sup> > hKv9.2-D379E* ( $p = 0.0001$ ).

**Expression of mutant Kv9.2-D379E significantly increases the firing frequency.** To test whether the hKv9.2-D379E subunit does indeed cause neuronal hyperexcitability, we performed current clamp recordings of clock neurons. We found that expression of hKv9.2-D379E subunit caused a significant increase in firing frequency (a measure of hyperexcitability) compared to expression of the hKv9.2 subunit (Fig. 4). The spontaneous action potential firing rate in flies expressing either hKv9.2 subunit was significantly different with the mutant subunit having a higher frequency ( $p = 0.0102$ ) (Fig. 4A,B). In order to further investigate the complex effects of expression of hKv9.2 and hKv9.2-D379E on Shab currents in *Drosophila* neurons, we developed a biophysical model that incorporated the major Kv currents separately. Major Kv current kinetics were fitted to the voltage-clamp data so that an accurate depiction of the specific effects of expression of hKv9.2 and hKv9.2-D379E subunits on the excitability of the whole-cell model could be determined. In particular, fitting the voltage clamp data (see Fig. 5) to classical Hodgkin-Huxley ionic current equations generated parameters consistent with the behaviors of flies with only native Shab or Shab perturbed by expression of hKv9.2 or hKv9.2-D379E on Shab (Fig. 5A,B). As illustrated in Fig. 6 the parameters obtained from the computational modeling are in concordance with experimental data. The hKv9.2 subunit activates at more negative values (activation  $V_h$ ) than the native Shab channel as observed in the experimental data. The extent of inactivation is also higher in hKv9.2-D379E in the model than in the wild type hKv9.2 flies as evidenced by the lower inactivation  $K$ . The speed of inactivation is also higher in the mutant hKv9.2-D379E as shown by the higher inactivation  $\sigma$ . Importantly, the spontaneous firing rate of action potentials obtained in whole-cell model simulations (i.e. after combining the individual ionic currents in a biophysical model of the electrical activity of the cell), in neurons expressing either the wild type or mutant hKv9.2 subunit agrees very well with the experimental (current clamp) data (Fig. 6).

**Expression of either hKv9.2 and hKv9.2-D379E causes a significant increase in night-time activity and reduction in sleep.** Sleep dysfunction, including short duration of sleep, has been reported in patients with ET<sup>31–33</sup>. To determine whether the neuronal hyperexcitability observed in hKv9.2 and hKv9.2-D379E in *Drosophila* affects circadian locomotor rhythms and sleep we characterized their circadian behavior.

While rhythmicity was unaffected by either hKv9.2 and hKv9.2-D379E channels (Table 1, Fig. 7), night-time activity was significantly increased ( $p = 0.02–0.0002$ ), and concurrently night-time sleep was reduced ( $p = 0.02–0.0001$ ) (Table 1, Fig. 8). Additionally, we observed a trend towards differences between hKv9.2 and hKv9.2-D379E channels (e.g. night-time sleep PDF  $>$  hKv9.2 vs PDF  $>$  hKv9.2-D379E  $p = 0.0745$  and night-time activity PDF  $>$  hKv9.2 vs PDF  $>$  hKv9.2-D379E  $p = 0.0913$ ), however the data did not reach statistical significance (Table 1). In sum, in addition to locomotor and electrophysiological defects, sleep is also disrupted by expression of hKv9.2 and hKv9.2-D379E channels in the *Drosophila* brain.

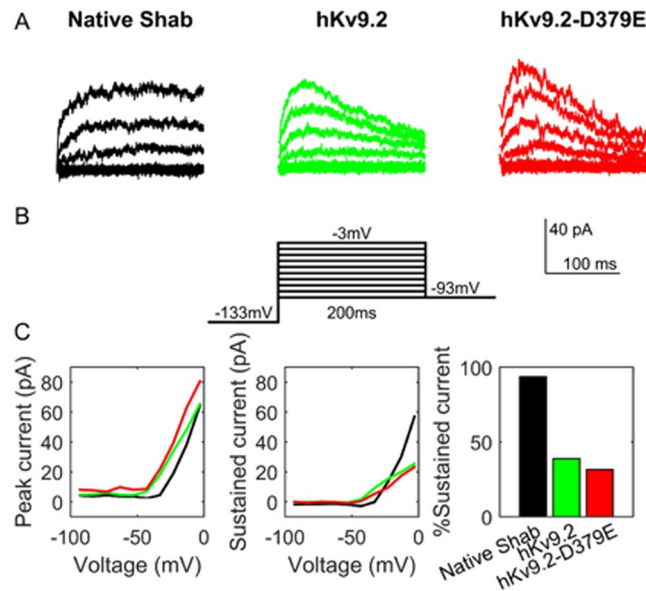


**Figure 3.** Expression of hKv9.2 or hKv9.2-D379E subunits causes an alteration in the kinetics of the native Shab (Kv2) channels. (A) Examples of the current evoked from *Drosophila* Shab when depolarized from  $-133$  mV to between  $-93$  mV and  $-3$  mV in flies expressing only native Shab (left panel), native Shab with the human Kv9.2 (middle panel), or native Shab with hKv9.2-D379E (right panel). The non-inactivating Shab becomes inactivating in the presence of either hKv9.2 subunit. (B) Diagram of the voltage step protocol used. (C) The I-V relationships for Shab determined from the three given genotypes. The peak current (left panel,  $n = 3$ ) shows that expression of either Kv9.2 subunit causes a shift in activation to more negative voltages. The sustained current (middle panel,  $n = 3$ ) shows that, at similar voltages, flies expressing either hKv9.2 subunit show reduced Shab current after 200 ms of depolarization. When the sustained current after 200 ms of depolarization to  $-3$  mV is expressed as a percentage of the peak current (right panel,  $n = 3$ ) the flies expressing only native Shab show high percentages, indicating very low levels of inactivation. When tested by two-way ANOVA, flies expressing either the wild-type hKv9.2 subunit ( $p < 0.001$ ) or the ET mutant hKv9.2-D379E subunit ( $p < 0.001$ ) were significantly different to flies expressing only native Shab. The mutant hKv9.2-D379E subunit shows much higher levels of inactivation than the wild-type hKv9.2 subunit ( $p = 0.0462$ ).

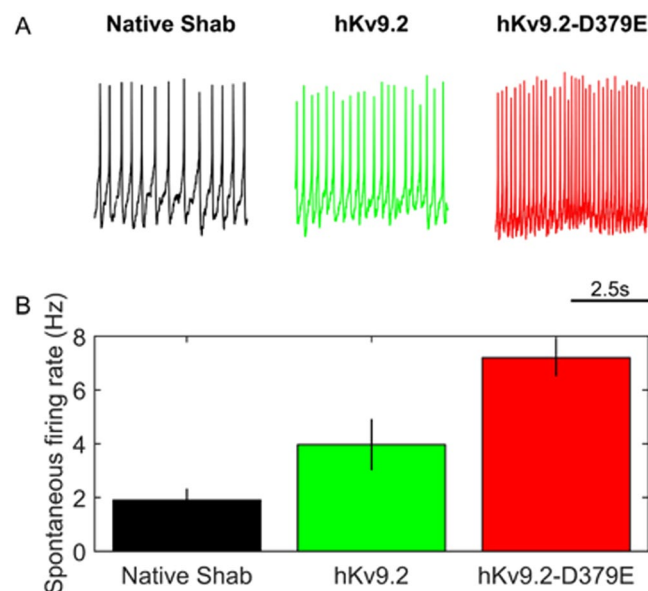


**Figure 4.** hKv9.2 subunits have significant and different impacts on resulting neuronal activity. (A) Representative example of 5 seconds of spontaneous activity in flies between ZT1 and ZT7 (where ZT0 is lights-on and ZT12 is lights-off) expressing only native Shab (left panel), native Shab with hKv9.2 (middle panel), or native Shab with hKv9.2-D379E (right panel). (B) The spontaneous firing rate of action potentials in flies expressing either hKv9.2 subunit (data are mean  $\pm$  S.D.,  $n = 3$ ) are significantly different with the mutant subunit having a higher frequency ( $t(4) = 5.3806$ ,  $p = 0.0102$ ).

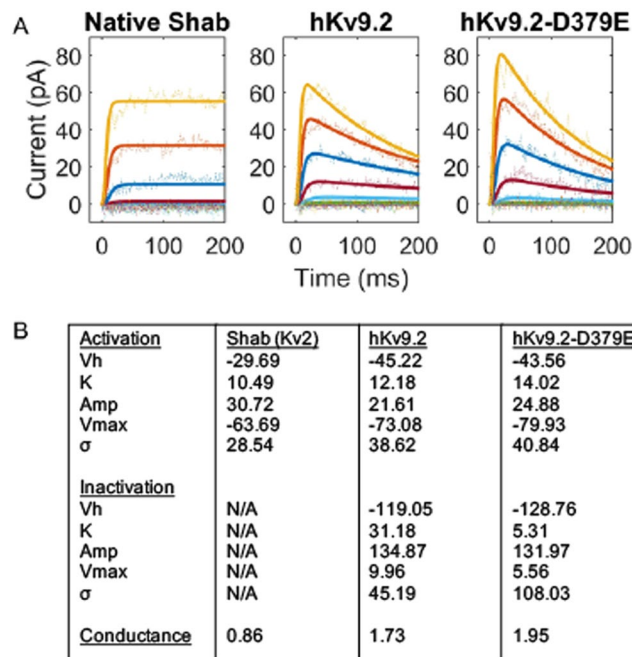


**Figure 5.** Computational models of Shab ion channel activity describe their differing kinetics. Fitting the electrophysiological data (see Fig. 1) to classical Hodgkin-Huxley equations generated parameters that describe the behaviors (**B**). These descriptions match well with experimental data acquired (**A**). The hKv9.2 subunits activate at more negative values (activation Vh) as seen in the experimental data. The extent of inactivation is higher in the mutant hKv9.2-D379E as evidenced by the lower inactivation K. The speed of inactivation is also higher in the mutant hKv9.2-D379E as shown by the higher inactivation  $\sigma$ .

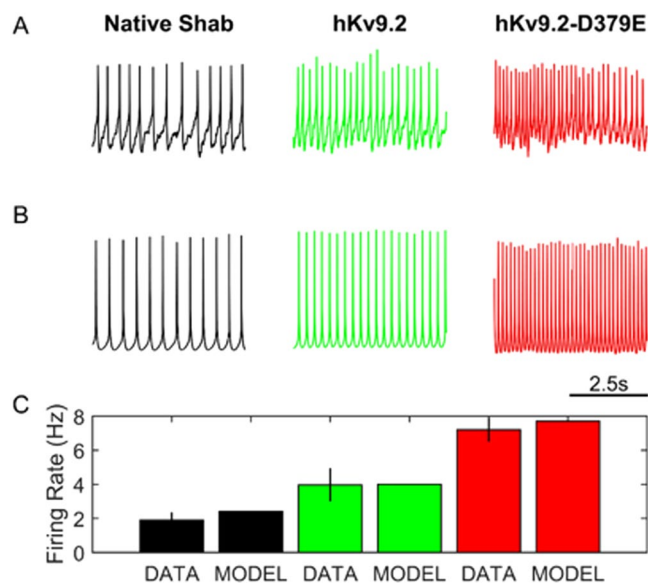


**Figure 6.** Whole cell computational models using hKv9.2 reflect changes in electrophysiological behavior. (**A**) Representative example of 5 seconds of spontaneous activity in flies expressing only native Shab (left panel), native Shab with hKv9.2 (middle panel), or native Shab with hKv9.2-D379E (right panel). (**B**) Model description of 5 seconds of neuronal activity using only native Shab (left panel), native Shab with hKv9.2 (middle panel), or native Shab with hKv9.2-D379E (right panel) at ZT0 (where ZT0 is lights-on/dawn and ZT12 is lights-off/dusk). (**C**) The model description of the spontaneous firing rate of action potentials in flies expressing either hKv9.2 subunit is not significantly different to the experimental data.

Control	Treatment	Assay	Control	Treatment	P-value
PDF	PDF-hKv9.2	Night-time sleep	0.7253 ± 0.0224	0.5576 ± 0.0239	<0.0001
hKv9.2	PDF-hKv9.2	Night-time sleep	0.7352 ± 0.0464	0.5576 ± 0.0239	0.0025
PDF	PDF-hKv9.2-D379E	Night-time sleep	0.7253 ± 0.0224	0.4901 ± 0.0271	<0.0001
hKv9.2-D379E	PDF-hKv9.2-D379E	Night-time sleep	0.6092 ± 0.0220	0.4901 ± 0.0271	0.0026
hKv9.2	TIM-hKv9.2	Night-time sleep	0.7352 ± 0.0464	0.5869 ± 0.0361	0.0178
hKv9.2-D379E	TIM-hKv9.2-D379E	Night-time sleep	0.6092 ± 0.0220	0.5228 ± 0.0202	0.0066
PDF	PDF-hKv9.2	Night-time activity	146.1510 ± 11.6796	224.4103 ± 16.3261	0.00036
hKv9.2	PDF-hKv9.2	Night-time activity	148.3000 ± 24.7850	224.4103 ± 16.3261	0.0199
PDF	PDF-hKv9.2-D379E	Night-time activity	146.1510 ± 11.6796	267.0952 ± 18.2757	<0.0001
hKv9.2-D379E	PDF-hKv9.2-D379E	Night-time activity	151.1019 ± 19.2544	267.0952 ± 18.2757	0.00032
hKv9.2	TIM-hKv9.2	Night-time activity	148.3000 ± 24.7850	242.0729 ± 35.4191	0.0403
hKv9.2-D379E	TIM-hKv9.2-D379E	Night-time activity	151.1019 ± 19.2544	263.7882 ± 16.1640	0.00023
hKv9.2	PDF-hKv9.2	Diurnal/nocturnal index	0.7116 ± 0.0387	0.3115 ± 0.0284	<0.0001
hKv9.2-D379E	PDF-hKv9.2-D379E	Diurnal/nocturnal index	0.4685 ± 0.0542	0.2861 ± 0.0466	0.02
hKv9.2	TIM-hKv9.2	Diurnal/nocturnal index	0.7116 ± 0.0387	0.4033 ± 0.0433	<0.0001
PDF-hKv9.2	PDF-hKv9.2-D379E	Night-time sleep	0.5576 ± 0.0239	0.4901 ± 0.0271	0.0745
PDF-hKv9.2	PDF-hKv9.2-D379E	Night-time activity	224.4103 ± 16.3261	267.0952 ± 18.2757	0.0913

**Table 1.** Night-time activity and sleep activity in flies expressing hKv9.2 and hKv9.2-D379E. Comparison of the analyzed data gathered in the *Drosophila* Activity Monitor (DAM). The comparison shows the data ± S.E.M. for each comparison (summarized in Figs 7 and 8) of night-time activity, night-time sleep, or the diurnal/nocturnal index.

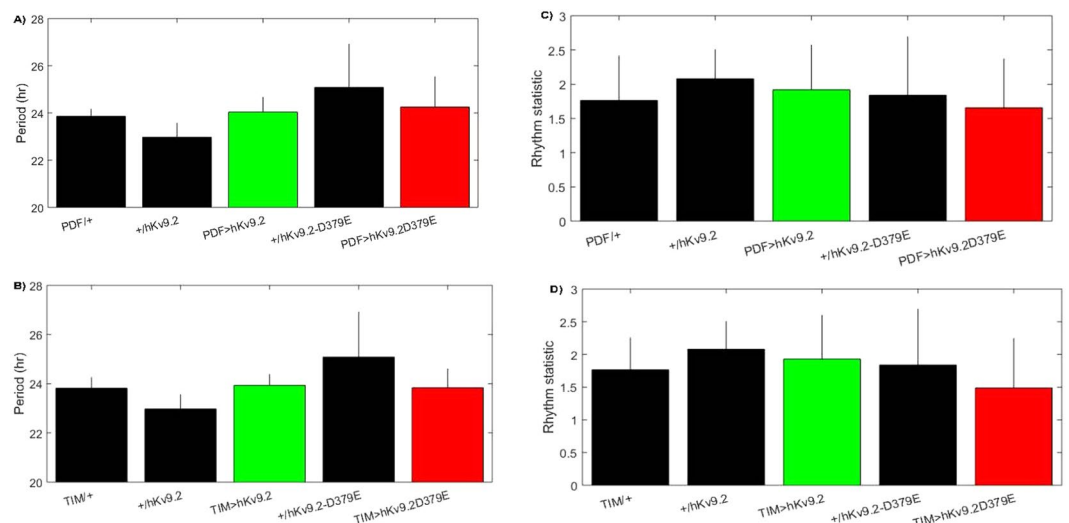


**Figure 7.** Effects of Expression of hKv9.2 and hKv9.2-D379E channels on Period or Rhythm Statistic. (A) Period of circadian locomotor rhythms in control flies and those expressing hKv9.2 or hKv9.2-D379E under the PDF promoter. (B) Period of circadian locomotor rhythms in control flies and those expressing hKv9.2 or hKv9.2-D379E under the TIM promoter. (C) The corresponding rhythm statistic obtained for flies using the PDF promoter. (D) The corresponding rhythm statistic obtained for flies using the TIM promoter.

## Discussion

We have created a model of ET by expressing the human Kv9.2 channel subunit in *Drosophila*. We show that the hKv9.2 subunit can modulate the endogenous Shab (Kv2 subfamily) channel activity. Behavioral manifestations of nervous system dysfunction consistent with a hyperexcitable phenotype were observed in flies expressing the hKv9.2 or hKv9.2-D379E subunit during development and in adult neurons only. Studying the effects of hKv9.2 and hKv9.2-D379E on CNS neuronal activity, we showed that the mutant hKv9.2-D379E subunit showed significantly higher levels of inactivation than the wild-type hKv9.2 subunit and a significantly higher frequency of spontaneous firing rate of action potentials consistent with neuronal hyperexcitability. A biophysical model of the electrical activity of the cell, combining the individual ionic currents in flies expressing hKv9.2 subunits, was in agreement with experimental data. Characterization of circadian behavior in flies expressing hKv9.2 and hKv9.2-D379E channels showed that while rhythmicity was unaffected significant differences were observed for night time activity and night time sleep. This is consistent with previous studies where hyperexcitation of lateral

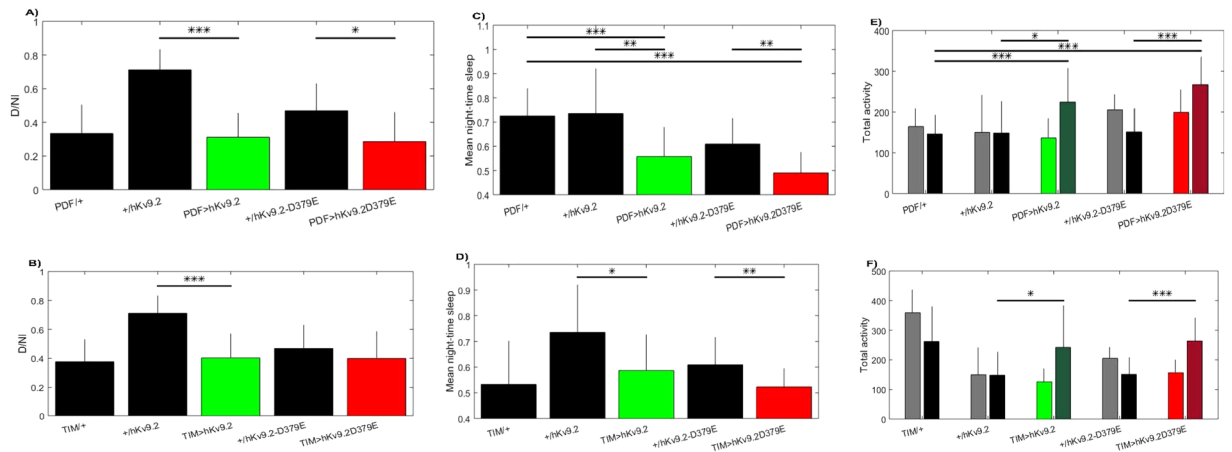


**Figure 8.** Effects of Expression of hKv9.2 and hKv9.2-D379E channels on diurnal/nocturnal index, average night time sleep and total night time activity. (**Top row**) Flies expressing hKv9.2 or hKv9.2-D379E under the PDF promoter and controls. (**Bottom row**) Flies expressing hKv9.2 or hKv9.2-D379E under the TIM promoter and controls. (**A,B**) The diurnal/nocturnal index (D/N I) examining the distribution of day-time and night-time activity. (**C,D**) The proportion of time flies spent asleep during the night-time, as defined as 5 minutes or more of inactivity. (**E,F**) The raw activity counts for flies split between day-time (lighter color, left-hand bars) and night-time (darker color, right-hand bars). Significant differences are observed in various comparisons summarized in Table 1.

ventral neurons by NaChBac (low-threshold voltage-gated sodium channel for hyperexcitation of the cell) caused an increase in night activity and decrease in night sleep<sup>34</sup> as seen in *Drosophila* models of Parkinson's disease<sup>35</sup>. While effects on period circadian protein have been seen<sup>36</sup>, no differences were seen in the current study.

While we recognise that there are limitations to the *Drosophila* model that we have developed because of the lack of a clear *Drosophila* ortholog for Kv9.2, our data is consistent with previous studies that have demonstrated that Kv9.2 modulates the activity of Kv2 channels<sup>2</sup> (such as *Drosophila* Shab), as well as observing significant differences in the phenotype (inactivation and spontaneous firing rate) between flies expressing the wild type and mutant hKv9.2 channels.

The pathogenicity of the KCNS2 mutation (p.D379E) that we identified in an early-onset ET family<sup>2</sup>, that is the focus of the current study, is further supported by functional data from the *Drosophila* model and is consistent with previous observations reported by us including co-segregation with ET in a family, prediction as a pathogenic amino acid substitution by several variant prediction tools, absence from population databases, and its location in the pore domain of the Kv9.2 channel.

Our data is consistent with recent reports and observations that ET may represent a family of disorders of neurological channelopathies, with mutations identified in a voltage-gated K<sup>+</sup> channel  $\alpha$  subunit (the focus of this study) in a family with pure ET<sup>2</sup>, in voltage-gated sodium channel  $\alpha$  subunits in a family with epilepsy and ET (SCN4A)<sup>37</sup> and a family with familial episodic pain and ET (SCN11A)<sup>38</sup>. Further, the T-type calcium channel, Ca<sub>v</sub>3, has been implicated in neuronal autorhythmicity<sup>39,40</sup> and is thought to underlie tremors seen in Parkinson's disease<sup>41</sup>, enhanced physiological tremor, and in ET<sup>42</sup> and T-type calcium channel antagonists have been shown to reduce tremor in mouse models of ET<sup>43,44</sup>. Nonetheless, the complete genetic basis for ET remains incomplete. Given the clinical and genetic heterogeneity observed in ET, further evaluation of ion channels as candidate genes for ET is warranted.

## Methods

**Transgenic *Drosophila*.** Human Kv9.2 sequenced-verified cDNA was obtained from the Mammalian Gene Collection (Clone ID: 5199736)(GE Dharmacon, Lafayette, Co). The RNA source for the cDNA was from an anonymous pool of 6 male brains, age range 23–27 years old. The library was oligo-dT primed and directionally cloned into pCMV-SPORT6 vector. Human Kv9.2 was transferred and cloned from the pCMV-SPORT6 vector by TOPO<sup>®</sup> cloning (ThermoFisher scientific, Waltham, MA) into the pBID-UAS *Drosophila* vector<sup>45</sup>.

Site directed mutagenesis was used to generate mutant human Kv9.2, c.1137 T > A, (p.D379E) using the Quick-change II site directed mutagenesis kit (Agilent Technologies, Santa Clara, CA) from the human Kv9.2 sequenced-verified cDNA. Germ-line transformants were generated with PhiC31 integrase with Chromosome II attP40 landing site. *Drosophila* were maintained with standard conditions and food. Uas-hKv9.2 and uas-hKv9.2-D379E were crossed to *Elav(c155)-Gal4* stock (Bloomington stock number-458) for pan-neural expression and *pdf-Gal4*, *pdf-rfp* for electrophysiological characterization<sup>29,30</sup>. Post-developmental effects utilized GAL80<sup>TS</sup> ro, restricting expression to adult neurons<sup>46–48</sup>. For electrophysiological and circadian analysis, expression was restricted to the LNV clock neurons by use of pdf-Gal4 or throughout the clock system through tim-Gal4.

**Western Blot Analysis.** An antibody to human Kv9.2 (Rabbit anti-Kv9.2, ThermoFisher PA5-29511) was used for Western blot analysis. The Kv9.2 antibody recombinant fragment corresponds to a region within amino acids 175–470 of human Kv9.2.

**Negative Geotaxis Climbing Assay.** The loss of climbing response was used to monitor ageing-related locomotor changes in *Drosophila*<sup>14,49</sup>. The climbing assay was performed as previously described<sup>14,49</sup>. We assessed 20 flies per vial for each transgenic and control line. Five trials were conducted for each vial. The average climbing rate was determined by measuring the time for the first fly to climb 17.5 cm. Climbing response was assessed at the following time points: Day 7, 14, 21, 28, 35, 42, 49, and 56.

*Expression of hKv9.2 and hKv9.2-D379E channels in adult neurons after development and effects on lifespan.* The climbing assay was performed as described for transgenic and control lines except 10 flies per vial were assessed for each line.

**Lifespan Assay.** Lifespan assays were performed as described previously<sup>50</sup>. Briefly, 200 virgin female flies per line were sex-segregated within 4 h of eclosion and maintained in small laboratory vials (n = 20 per vial) containing fresh food in a low-temperature incubator at 25 °C and 40% humidity on a 12/12 h dark/light cycle. The flies were then transferred to fresh food vials every 2–3 days and mortality recorded.

*Expression of hKv9.2 and hKv9.2-D379E channels in adult neurons after development and effects on lifespan.* A total of 100 flies per line were sex-segregated within 4 h of eclosion and age-matched flies were maintained in small laboratory vials (n = 10 per vial) containing fresh food in a high-temperature incubator at 29 °C and 40% humidity on a 12/12 h dark/light cycle. The flies were then transferred to fresh food vials every 2–3 days and mortality recorded.

**Anesthetization Induced Leg Shaking and Wing Scissoring Behavior.** Adult flies were anesthetized with ether and examined for leg shaking and wing scissoring as described previously<sup>23,24</sup>.

**Abnormal Wing Posture and Behavior Analyses.** For abnormal wing posture analysis, flies were aged as in the lifespan assays. The abnormal wing posture penetrance was calculated as the percentage of flies with elevated or drooped wing posture. For each experiment, at least 10 flies were scored for their wing posture phenotype for each genotype.

**Electrophysiology.** Experiments were conducted on wild type control: *pdf-Gal4; pdf-rfp*, as well as the two experimental lines: *pdf-Gal4 > uas-hKv9.2; pdf-rfp* and *pdf-Gal4/uas-hKv9.2-D379E; pdf-rfp*. Flies were housed in 12 h light: 12 h dark cycles to facilitate recordings throughout the day. All flies were raised at 25 °C (incubators) at humidity of 60%.

Whole fly brains were dissected from CO<sub>2</sub> anaesthetized adult flies aged between 0–5 days post-eclosion just before patch clamping using a previously established protocols<sup>29,30</sup>. Dissections were conducted in standard *Drosophila* external solution. The brain was then transferred to a recording chamber and held in place using a brain harp.

Whole-cell and patch-clamp recordings were made from the red fluorescent protein (RFP)-tagged pigment dispersing factor (PDF)-positive large Lateral Neuron ventral (l-LNv) clock neurons using a Multiclamp 700B amplifier and Axon Digidata 1440A digitizer in a recording chamber filled with *Drosophila* external solution as described previously<sup>29,30</sup>. Glass pipettes (8–15 MΩ) were pulled using a Sutter P-1000 puller and filled with internal solution. The resulting signal was then monitored and recorded using pClamp10 Clampex software and pipette offsets were zeroed prior to cell contact with the pipette capacitance being compensated upon contact. Subsequent signals were passed through a 10 kHz low-pass Bessel filter and sampled at 20 kHz. The cell-attached configuration was established by gentle suction applied through the pipette holder, and subsequent whole-cell configurations utilized a stronger pulse of negative pressure to break into the cell through the membrane.

The standard *Drosophila* external solution consisted of (in mM) 101 NaCl, 1 CaCl<sub>2</sub>, 4 MgCl<sub>2</sub>, 3 KCl, 5 glucose, 1.25 NaH<sub>2</sub>PO<sub>4</sub>, and 20.7 NaHCO<sub>3</sub> with pH 7.2 and osmolality 250 mOsm. The internal solution consisted of (in mM) 102 K-gluconate, 0.085 CaCl<sub>2</sub>, 1.7 MgCl<sub>2</sub>, 17 NaCl, 0.94 EGTA, and 8.5 HEPES with pH 7.2 and osmolality 235 mOsm. The pH was increased with NaOH for the external solution and KOH for the internal solution and decreased with HCl for both. Stock solutions of guangxitoxin-1E (GxTX, Alomone labs) were made up using external solution. The resulting junction potential for these solutions has been calculated as being –13 mV (data shown has been adjusted to account for this). During the recordings, the drug solutions are added by pipette to 1 ml of external solution in the recording chamber to achieve the final drug concentration.

Voltage-clamp recordings were initially held at a membrane potential of –93 mV. For I–V relationships, a standardized protocol was used consisting of a hyperpolarizing step of –40 mV to –133 mV for 500 ms and then steps in increments of 10 mV from –93 mV to –3 mV for a duration of 200 ms before a return to the holding potential of –80 mV. To measure Shab currents, voltage-clamp recordings were performed before and after application of 10 nM GxTX<sup>51</sup>, the difference between the two conditions gives the subtractive Shab current. Wash-out of the drug recovered the channel current (88.64% ± 3.06%).

***Drosophila* Activity Monitor (DAM).** Monitoring of the circadian activity of *Drosophila* was performed by measuring the locomotion of individual flies in a *Drosophila* activity monitor (DAM, Trikinetics Inc USA) system<sup>52</sup>. Male flies were initially held in 5 days of 12:12 LD (light/dark) before release into 7 days of DD (constant darkness). Analysis of activity was performed in Matlab and tubes showing no activity or early death were excluded from the analysis.

**Computational modeling.** Computational models of the Shab channel ionic current, with addition of hKv9.2 or hKv9.2-D379E channels were generated by a nonlinear optimization algorithm fitting the electrophysiological data to Hodgkin-Huxley equations<sup>53</sup> of the form:

$$I = gmax \times (m^P \times h^Q) \times (Vt - E) \quad (1)$$

where the current,  $I$ , depends on the maximal conductance ( $gmax$ ), the reversal potential of the channel ( $E$ ), the membrane voltage ( $Vt$ ), and the activation and inactivation ion channel gating variables ( $m$  and  $h$ ). The gating variables are given by the equations:

$$\frac{dm}{dt} = \frac{m_{\infty} - m}{\tau_m}, \quad (2)$$

$$m_{\infty} = \frac{1}{1 + e^{\frac{V-Vh}{k}}}, \quad (3)$$

$$\tau_m = Amp \times e^{-\frac{V-Vmax}{\sigma}} \quad (4)$$

$$\frac{dh}{dt} = \frac{h_{\infty} - h}{\tau_h}, \quad (5)$$

$$h_{\infty} = \frac{1}{1 + e^{\frac{V-Vh}{k}}}, \quad (6)$$

$$\tau_h = Amp \times e^{-\frac{V-Vmax}{\sigma}} \quad (7)$$

The individual ionic current models fitted to our data were then combined in a model of the electrical behavior of the whole cell. The resulting whole-cell computational model builds upon a previous model of suprachiasmatic nucleus (SCN) clock neurons<sup>54</sup> which incorporates  $Na^+$ ,  $K^+$ ,  $Ca^{2+}$ , and leak currents. However, in our model the original composite  $K^+$  current is separated into the four currents mediated via the major voltage-gated  $K^+$  channels (Shaker Kv1, Shab Kv2, Shaw Kv3 and Shal Kv4) found in the l-LNvs based on electrophysiological recordings; while Kv2 refers to either the native Shab current, native Shab with human hKv9.2, or native Shab with hKv9.2-D379E. The current balance equation then is:

$$C \frac{dV}{dt} = I_{app} - g_{Na} m^3 h (V - E_{Na}) - g_{Ca} m h (V - E_{Ca}) - g_{K1} m^4 h (V - E_K) - g_{K2} m^4 h (V - E_K) - g_{K4} m^4 h (V - E_K) - g_{K3} m^4 h (V - E_K) - g_{leak} (V - E_{leak}) \quad (8)$$

where  $E_{Na} = 52$  mV,  $E_{Ca} = 132$  mV,  $E_K = -90$  mV, and  $E_{leak} = -7$  mV are the reversal potentials. These were calculated using the Nernst and Goldman-Hodgkin-Katz voltage equations based on the internal and external solutions used.

**Statistical Analysis.** Statistical analysis was carried out using the Prism 7.0 (GraphPad Software, Inc., La Jolla, CA) software. Analysis of climbing response during lifespan was performed using unpaired student's t-test (one unpaired t-test per row) in Prism 7.0. Data were represented as the mean and standard error of the mean (S.E.M.) from at least ten independent experiments at each week. Comparisons included *Elav/+* versus *Elav > hKv9.2*, *Elav/+* versus *Elav > hKv9.2-D379E* and *Elav > hKv9.2* versus *Elav > hKv9.2-D379E*. The false discovery rate (FDR) approach method used was the two-stage step up method of Benjamini, Krieger and Yekutieli (FDR (Q) = 1%). Comparison of survival curves was performed using the Log-rank (Mantel Cox) test and the Gehan-Breslow-Wilcoxon test in Prism 7.0. Analysis of electrophysiology data was performed using pClamp10 Clampfit software and Matlab (Mathworks).

**Data availability.** The authors declare that all data supporting the findings of this study are available within this article. Supplementary information files are available from the corresponding authors upon reasonable request.

## References

- Louis, E. D. Re-thinking the biology of essential tremor: from models to morphology. *Parkinsonism Relat Disord* **20**(Suppl 1), S88–93, [https://doi.org/10.1016/S1353-8020\(13\)70023-3](https://doi.org/10.1016/S1353-8020(13)70023-3) (2014).
- Liu, X. *et al.* Identification of candidate genes for familial early-onset essential tremor. *European journal of human genetics: EJHG*, <https://doi.org/10.1038/ejhg.2015.228> (2015).
- Salinas, M., Duprat, F., Heurteaux, C., Hugnot, J. P. & Lazdunski, M. New modulatory alpha subunits for mammalian Shab K<sup>+</sup> channels. *J Biol Chem* **272**, 24371–24379 (1997).
- Ueda, A. & Wu, C. F. Distinct frequency-dependent regulation of nerve terminal excitability and synaptic transmission by IA and IK potassium channels revealed by *Drosophila* Shaker and Shab mutations. *J Neurosci* **26**, 6238–6248, <https://doi.org/10.1523/JNEUROSCI.0862-06.2006> (2006).

5. Covarrubias, M., Wei, A. A. & Salkoff, L. Shaker, Shal, Shab, and Shaw express independent K<sup>+</sup> current systems. *Neuron* **7**, 763–773 (1991).
6. Tsunoda, S. & Salkoff, L. Genetic analysis of *Drosophila* neurons: Shal, Shaw, and Shab encode most embryonic potassium currents. *J Neurosci* **15**, 1741–1754 (1995).
7. Peers, C. & Boyle, J. P. Oxidative modulation of K<sup>+</sup> channels in the central nervous system in neurodegenerative diseases and aging. *Antioxid Redox Signal* **22**, 505–521, <https://doi.org/10.1089/ars.2014.6007> (2015).
8. Klein, A., Boltshauser, E., Jen, J. & Baloh, R. W. Episodic ataxia type 1 with distal weakness: a novel manifestation of a potassium channelopathy. *Neuropediatrics* **35**, 147–149, <https://doi.org/10.1055/s-2004-817921> (2004).
9. Waters, M. F. *et al.* Mutations in voltage-gated potassium channel KCNC3 cause degenerative and developmental central nervous system phenotypes. *Nature genetics* **38**, 447–451, <https://doi.org/10.1038/ng1758> (2006).
10. Matsukawa, H., Wolf, A. M., Matsushita, S., Joho, R. H. & Knopfel, T. Motor dysfunction and altered synaptic transmission at the parallel fiber-Purkinje cell synapse in mice lacking potassium channels Kv3.1 and Kv3.3. *J Neurosci* **23**, 7677–7684 (2003).
11. McMahon, A. *et al.* Allele-dependent changes of olivocerebellar circuit properties in the absence of the voltage-gated potassium channels Kv3.1 and Kv3.3. *Eur J Neurosci* **19**, 3317–3327, <https://doi.org/10.1111/j.0953-816X.2004.03385.x> (2004).
12. Espinosa, F., Marks, G., Heintz, N. & Joho, R. H. Increased motor drive and sleep loss in mice lacking Kv3-type potassium channels. *Genes Brain Behav* **3**, 90–100 (2004).
13. Kumar, P., Kumar, D., Jha, S. K., Jha, N. K. & Ambasta, R. K. Ion Channels in Neurological Disorders. *Adv Protein Chem Struct Biol* **103**, 97–136, <https://doi.org/10.1016/bs.apcsb.2015.10.006> (2016).
14. Le Bourg, E. & Lints, F. A. Hypergravity and aging in *Drosophila melanogaster*. 4. Climbing activity. *Gerontology* **38**, 59–64 (1992).
15. Cirelli, C. *et al.* Reduced sleep in *Drosophila* Shaker mutants. *Nature* **434**, 1087–1092, <https://doi.org/10.1038/nature03486> (2005).
16. Bushey, D., Huber, R., Tononi, G. & Cirelli, C. *Drosophila* Hyperkinetic mutants have reduced sleep and impaired memory. *J Neurosci* **27**, 5384–5393, <https://doi.org/10.1523/JNEUROSCI.0108-07.2007> (2007).
17. Louis, E. D., Benito-Leon, J., Ottman, R. & Bermejo-Pareja, F. Neurological Disorders in Central Spain Study, G. A population-based study of mortality in essential tremor. *Neurology* **69**, 1982–1989, <https://doi.org/10.1212/01.wnl.0000279339.87987.d7> (2007).
18. Bonini, N. M. A genetic model for human polyglutamine-repeat disease in *Drosophila melanogaster*. *Philos Trans R Soc Lond B Biol Sci* **354**, 1057–1060, <https://doi.org/10.1098/rstb.1999.0458> (1999).
19. Park, J. *et al.* Mitochondrial dysfunction in *Drosophila* PINK1 mutants is complemented by parkin. *Nature* **441**, 1157–1161, <https://doi.org/10.1038/nature04788> (2006).
20. Greene, J. C. *et al.* Mitochondrial pathology and apoptotic muscle degeneration in *Drosophila* parkin mutants. *Proc Natl Acad Sci USA* **100**, 4078–4083, <https://doi.org/10.1073/pnas.0737556100> (2003).
21. Flood, T. F., Gorczyca, M., White, B. H., Ito, K. & Yoshihara, M. A large-scale behavioral screen to identify neurons controlling motor programs in the *Drosophila* brain. *G3 (Bethesda)* **3**, 1629–1637, <https://doi.org/10.1534/g3.113.006205> (2013).
22. Engel, J. E. & Wu, C. F. Interactions of membrane excitability mutations affecting potassium and sodium currents in the flight and giant fiber escape systems of *Drosophila*. *J Comp Physiol A* **171**, 93–104 (1992).
23. Kaplan, W. D. & Trout, W. E. 3rd The behavior of four neurological mutants of *Drosophila*. *Genetics* **61**, 399–409 (1969).
24. Wang, J. W., Humphreys, J. M., Phillips, J. P., Hilliker, A. J. & Wu, C. F. A novel leg-shaking *Drosophila* mutant defective in a voltage-gated K<sup>(+)</sup> current and hypersensitive to reactive oxygen species. *J Neurosci* **20**, 5958–5964 (2000).
25. Hodge, J. J., Choi, J. C., O’Kane, C. J. & Griffith, L. C. Shaw potassium channel genes in *Drosophila*. *J Neurobiol* **63**, 235–254, <https://doi.org/10.1002/neu.20126> (2005).
26. Reddy, R. V. *et al.* Excitatory effects and electroencephalographic correlation of etomidate, thiopental, methohexital, and propofol. *Anesth Analg* **77**, 1008–1011 (1993).
27. Jankovic, J., Beach, J., Pandolfo, M. & Patel, P. I. Familial essential tremor in 4 kindreds. Prospects for genetic mapping. *Arch Neurol* **54**, 289–294 (1997).
28. Richter, A. *et al.* The “campus syndrome” in pigs: neurological, neurophysiological, and neuropharmacological characterization of a new genetic animal model of high-frequency tremor. *Exp Neurol* **134**, 205–213, <https://doi.org/10.1006/exnr.1995.1050> (1995).
29. Chen, C. *et al.* *Drosophila* Ionotropic Receptor 25a mediates circadian clock resetting by temperature. *Nature* **527**, 516–520, <https://doi.org/10.1038/nature16148> (2015).
30. Buhl, E. *et al.* Quasimodo mediates daily and acute light effects on *Drosophila* clock neuron excitability. *Proc Natl Acad Sci USA* **113**, 13486–13491, <https://doi.org/10.1073/pnas.1606547113> (2016).
31. Benito-Leon, J., Louis, E. D. & Bermejo-Pareja, F. Short sleep duration heralds essential tremor: a prospective, population-based study. *Mov Disord* **28**, 1700–1707, <https://doi.org/10.1002/mds.25590> (2013).
32. Rohl, B. *et al.* Daytime sleepiness and nighttime sleep quality across the full spectrum of cognitive presentations in essential tremor. *J Neurol Sci* **371**, 24–31, <https://doi.org/10.1016/j.jns.2016.10.006> (2016).
33. Lenka, A., Benito-Leon, J. & Louis, E. D. Is there a Premotor Phase of Essential Tremor? *Tremor Other Hyperkinet Mov (N Y)* **7**, 498, <https://doi.org/10.7916/D80S01VK> (2017).
34. Sheeba, V. *et al.* Large ventral lateral neurons modulate arousal and sleep in *Drosophila*. *Curr Biol* **18**, 1537–1545, <https://doi.org/10.1016/j.cub.2008.08.033> (2008).
35. Julienne, H., Buhl, E., Leslie, D. S. & Hodge, J. J. L. *Drosophila* PINK1 and parkin loss-of-function mutants display a range of non-motor Parkinson’s disease phenotypes. *Neurobiol Dis* **104**, 15–23, <https://doi.org/10.1016/j.nbd.2017.04.014> (2017).
36. Nitabach, M. N. *et al.* Electrical hyperexcitation of lateral ventral pacemaker neurons desynchronizes downstream circadian oscillators in the fly circadian circuit and induces multiple behavioral periods. *J Neurosci* **26**, 479–489, <https://doi.org/10.1523/JNEUROSCI.3915-05.2006> (2006).
37. Bergareche, A. *et al.* SCN4A pore mutation pathogenetically contributes to autosomal dominant essential tremor and may increase susceptibility to epilepsy. *Human molecular genetics*, <https://doi.org/10.1093/hmg/ddv410> (2015).
38. Leng, X. R., Qi, X. H., Zhou, Y. T. & Wang, Y. P. Gain-of-function mutation p.Arg225Cys in SCN11A causes familial episodic pain and contributes to essential tremor. *J Hum Genet* **62**, 641–646, <https://doi.org/10.1038/jhg.2017.21> (2017).
39. Llinas, R. R. The intrinsic electrophysiological properties of mammalian neurons: insights into central nervous system function. *Science* **242**, 1654–1664 (1988).
40. Perez-Reyes, E. Molecular physiology of low-voltage-activated t-type calcium channels. *Physiol Rev* **83**, 117–161, <https://doi.org/10.1152/physrev.00018.2002> (2003).
41. Sarnthein, J. & Jeanmonod, D. High thalamocortical theta coherence in patients with Parkinson’s disease. *J Neurosci* **27**, 124–131, <https://doi.org/10.1523/JNEUROSCI.2411-06.2007> (2007).
42. Filip, P., Lungu, O. V., Manto, M. U. & Bares, M. Linking Essential Tremor to the Cerebellum: Physiological Evidence. *Cerebellum* **15**, 774–780, <https://doi.org/10.1007/s12311-015-0740-2> (2016).
43. Sinton, C. M., Krosser, B. I., Walton, K. D. & Llinas, R. R. The effectiveness of different isomers of octanol as blockers of harmaline-induced tremor. *Pflugers Arch* **414**, 31–36 (1989).
44. Handforth, A. Harmaline tremor: underlying mechanisms in a potential animal model of essential tremor. *Tremor Other Hyperkinet Mov (N Y)* **2**, <https://doi.org/10.7916/D8TD9W2P> (2012).
45. Wang, J. W., Beck, E. S. & McCabe, B. D. A modular toolset for recombination transgenesis and neurogenetic analysis of *Drosophila*. *PLoS One* **7**, e42102, <https://doi.org/10.1371/journal.pone.0042102> (2012).

46. Nogi, Y., Matsumoto, K., Toh-e, A. & Oshima, Y. Interaction of super-repressible and dominant constitutive mutations for the synthesis of galactose pathway enzymes in *Saccharomyces cerevisiae*. *Mol Gen Genet* **152**, 137–144 (1977).
47. Nogi, Y., Shimada, H., Matsuzaki, Y., Hashimoto, H. & Fukasawa, T. Regulation of expression of the galactose gene cluster in *Saccharomyces cerevisiae*. II. The isolation and dosage effect of the regulatory gene GAL80. *Mol Gen Genet* **195**, 29–34 (1984).
48. Lue, N. F., Chasman, D. I., Buchman, A. R. & Kornberg, R. D. Interaction of GAL4 and GAL80 gene regulatory proteins *in vitro*. *Mol Cell Biol* **7**, 3446–3451 (1987).
49. Ganetzky, B. & Flanagan, J. R. On the relationship between senescence and age-related changes in two wild-type strains of *Drosophila melanogaster*. *Exp Gerontol* **13**, 189–196 (1978).
50. Linford, N. J., Bilgir, C., Ro, J. & Pletcher, S. D. Measurement of lifespan in *Drosophila melanogaster*. *J Vis Exp*. <https://doi.org/10.3791/50068> (2013).
51. Herrington, J. *et al.* Blockers of the delayed-rectifier potassium current in pancreatic beta-cells enhance glucose-dependent insulin secretion. *Diabetes* **55**, 1034–1042 (2006).
52. Schlichting, M. & Helfrich-Forster, C. Photic entrainment in *Drosophila* assessed by locomotor activity recordings. *Methods Enzymol* **552**, 105–123. <https://doi.org/10.1016/bs.mie.2014.10.017> (2015).
53. Hodgkin, A. L. & Huxley, A. F. A quantitative description of membrane current and its application to conduction and excitation in nerve. *J Physiol* **117**, 500–544 (1952).
54. Belle, M. D., Diekman, C. O., Forger, D. B. & Piggins, H. D. Daily electrical silencing in the mammalian circadian clock. *Science* **326**, 281–284. <https://doi.org/10.1126/science.1169657> (2009).

## Acknowledgements

This work was supported by a grant from the National Institutes of Health, R01NS073872, to L.N.C and E.D.L. The electrophysiology was supported by a grant from the Biotechnology and Biological Sciences Research Council South West Biosciences, United Kingdom, DTP BB/J014400/1 to J.J.L.H. K.T.-A. gratefully acknowledges the financial support of the Engineering and Physical Sciences Research Council via Grant No. EP/N014391/1.

## Author Contributions

Cloning, mutagenesis and generation of hKv9.2 transgenic *Drosophila* lines was performed by R.A., L.N.C. and B.D.M. Western blot analysis was performed by S.S., L.N.C. and I.S.-M. Phenotyping and behavioral assays including locomotor assays, lifespan assays, anesthetization induced leg shaking and wing scissoring behavior, and abnormal wing posture analyses was performed by R.A., L.N.C., I.S.-M., B.D.M., Z.O. and E.D.L. Electrophysiology and circadian rhythm and sleep behavioral analysis was performed by P.S. and J.J.L.H. Computational modeling was performed by P.S. and K.T.-A. Statistical analyses was performed by L.N.C., P.S., J.J.L.H. and K.T.-A. L.N.C., B.D.M., J.J.L.H. and K.T.-A. designed the study and wrote the paper. All authors discussed the results and provided critical evaluation and comments on the manuscript. Funding for the study was provided by L.N.C., E.D.L., J.J.L.H., and K.T.-A.

## Additional Information

**Supplementary information** accompanies this paper at <https://doi.org/10.1038/s41598-018-25949-w>.

**Competing Interests:** The authors declare no competing interests.

**Publisher's note:** Springer Nature remains neutral with regard to jurisdictional claims in published maps and institutional affiliations.



**Open Access** This article is licensed under a Creative Commons Attribution 4.0 International License, which permits use, sharing, adaptation, distribution and reproduction in any medium or format, as long as you give appropriate credit to the original author(s) and the source, provide a link to the Creative Commons license, and indicate if changes were made. The images or other third party material in this article are included in the article's Creative Commons license, unless indicated otherwise in a credit line to the material. If material is not included in the article's Creative Commons license and your intended use is not permitted by statutory regulation or exceeds the permitted use, you will need to obtain permission directly from the copyright holder. To view a copy of this license, visit <http://creativecommons.org/licenses/by/4.0/>.

© The Author(s) 2018